Influence of desiccation cracking on the liquefaction Potential of Thickened Tailing Deposits

G. Barrios, E. Sáez & C. Ledezma
Pontificia Universidad Católica de Chile, College of Engineering, Department of Structural and Geotechnical Engineering

SUMMARY:
Copper production is an essential component of Chilean economy. During copper's extraction process, large quantities of waste materials (tailings) are produced, which are typically stored in large tailing ponds. Thickened Tailings Deposits (TTDs) are an alternative to conventional tailings ponds. In TTDs a considerable amount of water is extracted from the tailings before their deposition, increasing the storage capacity of the deposit and eventually improving its seismic stability. Once a thickened tailings layer is deposited, it loses water and it shrinks, forming a relatively regular structure of tailings' blocks with vertical cracks in between, which are then filled up with "fresh" tailings coming from the upper layer.
The dynamic response of this complex structure made of "solid" blocks with softer material in between was analyzed using an inelastic fully coupled dynamic hydro-mechanic finite element approach. The tailings behaviour was modelled using an elasto-plastic multi-yielding constitutive model, which parameters were calibrated using experimental data. Random field theory was used to generate realistic desiccation cracking patterns compatible with some field observation.

Keywords: thickened tailings, liquefaction assessment, desiccation cracks, numerical modelling.

1. INTRODUCTION

In Chilean copper mines, about 1% by weight of the extracted rock is ore. As a consequence, there are large quantities of waste materials (tailings) that have to be safely stored. Indeed, more than one million of tons of tailings are disposed every day in Chile. Given the composition and high water content of conventional tailings, this type of deposits may be adversely affected by medium to strong seismic ground motions. Past earthquakes have shown that inadequate practices may lead to failure of these deposits, causing spillage of thousands of cubic meters of tailings, serious environmental consequences, and even causalities. For instance, in the M 7.4 Chilean earthquake of March 28, 1965, eight tailings dams failed. Two of them destroyed El Cobre town and killed more than 200 people.
There are several ways to store tailings. In conventional tailings dams, Chile's most common choice, the retaining wall is build using the coarser fraction of the tailings material. There are other alternatives to conventional deposits; one of these is the Thickened Tailings Disposal (TTD). In TTD a considerable amount of water is extracted from the tailings before their deposition, increasing the storage capacity of the deposit and its seismic stability (Robinsky, 1999). Another advantage of this system is that smaller dams are needed to contain a given mass of tailings. Thickened tailings form a "self-supporting" structure that can be placed even on nearly flat terrain without dams. On the other hand, some of the disadvantages of this technique are the uncertainty on the evolution of tailings' properties with time (e.g., oxidation), its 1liquefaction susceptibility, the difficulty of predicting the angle of the tailings deposit, and the acid drainage potential. Therefore, in certain circumstances a more conventional tailings' system will prove preferable.

TTDs have only been implemented in medium-sized mining projects and in areas with rather low seismic activity. The use of this deposition technique in countries like Chile, with large mining projects and high seismicity, needs to be thoroughly evaluated before its implementation in actual projects. Usually, numerical models consider thickened tailings as a homogenous material with equivalent properties. However, these models do not represent the actual structure of a thickened tailings deposit. Once a thickened tailing layer is deposited it loses water and it shrinks, forming a relatively regular structure of tailings' blocks with vertical cracks in between. When a new tailings layer is deposited, the vertical cracks are filled up with "fresh" tailings, which do not reach the shrinkage limit. Then, thickened tailings deposits forms a structure made of "solid" blocks with softer material in between (Figure 1). Cracks widths range from a few millimetres to as much 50 mm, depending on the size and mineralogy of the tailings particles.

The main objective of this study was to evaluate the seismic behavior and liquefaction potential of a thickened tailings deposit, by adding tailings cracks into a two-dimensional plane-strain numerical model. Pore water pressure build-up distribution was evaluated for a realization of randomly distributed cracks. For this study, liquefaction is defined as the substantial loss of shear strength of medium to low permeability saturated loose granular soils under cyclic shear loading. This phenomenon is triggered by the contracting tendency of loose materials which induce pore pressure build-up and consequent effective stress reduction. Earthquakes induced liquefaction has been observed in several tailings dams throughout the world (Verdugo 2009, 2011).

Figure 1. Typical desiccation crack pattern observed in a TTD in Chile

Figure 2. General overview of a TTD in Chile

2. MODELING APPROACH

A fully coupled hydro-mechanical dynamical approach was usd to model the thickened tailing deposit. We adopted the u_s – p formulation (Zienkiewicz, 1984) that neglects the relative fluid to soil acceleration terms, which is a reasonable assumption for earthquake-engineering's typical frequency ranges of analysis. With this simplification, the unknown variables are the displacement of the solid u_s and the pore pressure of the water *p*. Additionally, soil grain compressibility is neglected and thermal effects are ignored.

2.1. Geometry

A thickened tailings deposit is a complex 3D structure (Figure 2), and a complete 3D numerical model would be computationally extremely expensive. Therefore, we generated a plane-strain 2D model representative of a vertical section of a typical TTD (Figure 3). The model considers a portion of the bedrock (1), the retaining dam (2) and the TTD (3). The 2D model assumes an elliptical truncation of the unbounded half-space elastic rock. In this boundary, paraxial elements simulating the deformable unbounded bedrock have been placed (Modaressi, 1994). These elements ensure the radiation damping condition and allow the inclusion of an arbitrary incident wave. A dam height of 20 m and a thickened deposit's length of 300 m were selected for the analysis. The TTD's free surface was assumed to be perfectly horizontal, with a variable thickness of 20 m to 30 m.

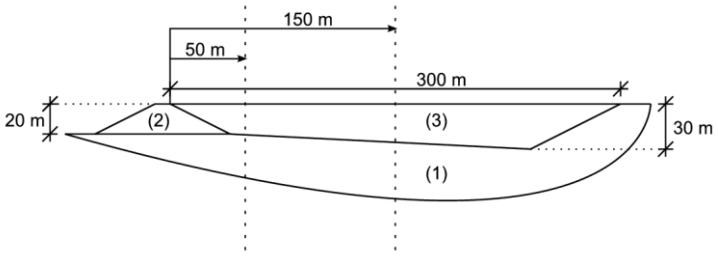

Figure 3. Outline of the geometry of the deposit.

2.2. Details of the FEM model

The plane-strain approach was used to represent a 2D section of the deposit. The generated FE model uses linear triangular elements for both displacements and pressures. The ECP's (Ecole Centrale de Paris) elasto-plastic cyclic multi-yielding constitutive model (Aubry, 1982 and Hujeux, 1985) was used to represent both the TTD (ML according to USCS classification system) and the rockfill dam behavior. The model' parameters for the deposit were calibrated using the results of the undrained triaxial tests performed by Cifuentes (2007) and calibrated by Ferrer (2011). Two set of parameters were defined, in order to reproduce the experimental behavior at mean pressures of 98 and 196 kPa (Table 2.1). Figures 4a and 4b show a reasonable agreement between numerical model estimations and experimental data. The parameters for the dam material were obtained from Nieto-Gamboa (2011). All FE analyzes were performed using the GEFDyn code (Aubry, 1996).

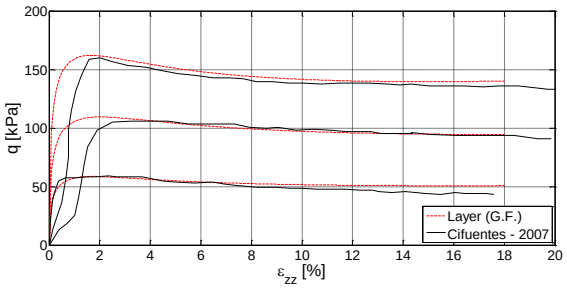

Figure 4a. q V/S axial strain (ε_{zz})

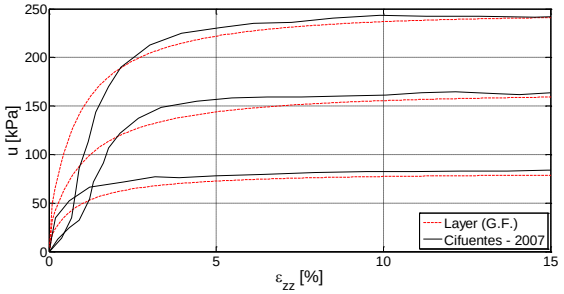

Figure 4b. Pore pressure V/S axial strain (ε_{zz})

Table 2.1. Parameters of the model used for the Thickened Tailing (TT)

Mean pressure	Friction angle (φ)	Dilatancy angle (ψ)	Plastic compressibility (β)	b	Initial mean pressure at critical state (p_c)
98 kPa	35°	35°	20	0.1	0.6E5
196 kPa	35°	35°	20	0.1	1.2E5

Where **b**=0 corresponds to a Mohr-Coulomb type yield surface, while **b**=1 corresponds to a Cam-Clay type yield surface.

2.3. Desiccation cracks

Actual desiccation cracks patterns of thickened tailings deposits are complex and they vary with depth and horizontal distance. For the in-plane crack growth pattern, Horgan & Youg, (1999) developed an empirical algorithm based in the random-walk problem. However, they could not get a final model that was able to reproduce the desiccation's propagation with depth.

To model this aspect of the phenomenon, we considered two different crack creation/propagation models. The first one is an independent process that goes from the bottom layer to the top one, horizontally dividing each layer by a fix parameter Δx that represents the minimum size of a solid block. We assigned a probability (α_1) to crack creation. Each crack is considered to propagate vertically, thus in the top of the same layer the crack propagation stops.

The second model assigns a probability (α_2) to the fact that each crack coming from a certain layer may propagates into the upper layer.

Finally we developed a compatibility procedure based on a minimum distance (l_{min}) between two adjacent cracks. We assumed that the propagation of the existing cracks is the dominant process; therefore, if a "new crack" from the first process exists at a distance inferior than l_{min} the crack arising from the second process prevails over the first one.

Figure 5 shows the result for layers 20cm high, with a minimum distance between cracks of 20 cm, and Δx=0.5 m.

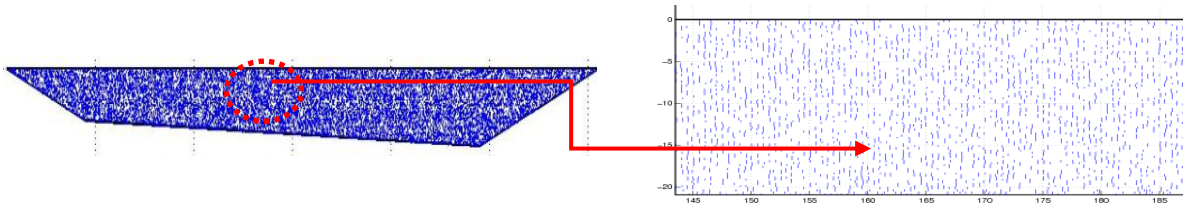

Figure 5a. Random crack pattern

Figure 5b. Zoom random crack pattern

To introduce this complex cracks' pattern into the FE model's mesh, compatibility criteria has to be used. First, we selected the FEM nodes and compared them with the independently generated crack pattern decide if each node was close enough (parameter d_{max}) to be a node inside a crack. If a node met this criterion, it was considered as a "crack node".

Then, we checked all the triangular elements of the model to see which ones were formed by two or more of these "crack nodes". This subset of elements was assigned corresponding material properties to properly define the crack pattern inside the TTD. Figure 6 shows the result of one random generation using this procedure.

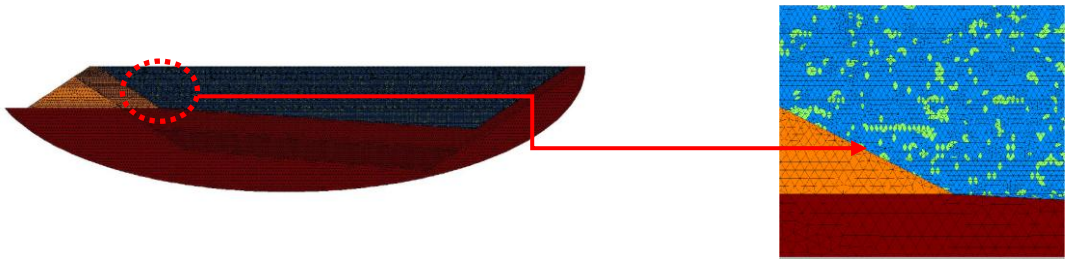

Figure 6a. Random crack pattern on FEM model

Figure 6b. Zoom random crack pattern on FEM model

To the authors' knowledge no experimental data about the mechanical behavior of the fresh material filling the crack has been published yet. Nevertheless, it seems reasonable to assume that this material would have a higher void ratio than the desiccated blocks because it has not been directly exposed to the ambient, which means that it has not had the opportunity to shrink too much. Hence and to simplify the inclusion of the fresh material in the model, we adopted a hydraulic conductivity for the fresh material equal to ten times that of the blocks, keeping all the others constitutive model parameters the same. There are probably other differences between the mechanical behavior of fresh material and that of desiccated and re-saturated material constituting the layers, e.g.: stiffness, solid skeleton compressibility, shear strength, etc. Nevertheless, and for the sake of simplicity we restricted the present study to permeability-related effects. In future stages of the research, we will explore the effects of other mechanical characteristics of fresh material.

3. MESH SENSITIVITY

Mesh size and the characteristic length of the elements are key issues when a wave-propagation problem is addressed. In general terms, a minimum of 8 to 10 elements per wavelength must be used to properly characterize a given wave. Depending on the stiffness of the material and the frequency range to be analyzed, this rule provides an initial estimation of elements' size. However, other restrictions must be considered to satisfactorily reproduce the pore pressure build-up and the fluid flows inside the TTD. When the desiccation cracks are added to the model, the elements' minimum size is strongly controlled by the geometric assumptions used to randomly generate the crack pattern, i.e., the average block size, the thickness of each layers, and the crack width. If the material is assumed to be homogeneous, there is still some freedom to choose a fine enough mesh that is able to reproduce the key aspects of the model. This section addresses this last issue, i.e., how to define a reasonably fine mesh for the reference homogeneous case.

Before performing any non-linear dynamic analysis, a compatible initial stress state must be obtained. With this purpose in mind, we simulated the construction of the pond in three global phases: initialization of the bedrock, simulation of the sequential construction of the dam, and deposition of the TT. This sequential construction simulation also results in a realistic deformation field. Figure 7 shows the result of this simulation. Note that since impervious mechanical interfaces were used between the tailings, the bedrock, and the rockfill. Stresses are discontinuous at the interface between the saturated tailings and the surrounding dry material. Also, sliding and contact loose are allowed between the tailings and the bedrock or the rockfill, but normal flows are null during both static and dynamical computations.

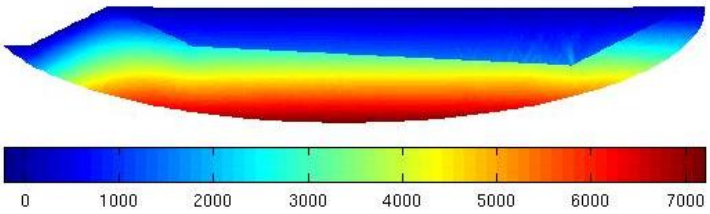

Figure 7. Initial vertical stress state distribution (kPa)

The final stress state of the static analysis is used as the initial stress state of the dynamic analysis. The seismic analysis is computed as a dynamical perturbation around the static equilibrium, thus no mechanical restrictions are required at the bottom boundary. The paraxial elements used to simulate the elastic half-space introduce the incoming wave as a time-dependent stress distribution on this boundary. This stress distribution is superimposed to the impedance stress-velocity relationship to satisfy the required radiation condition.
The effect of the mesh size was studied for the homogeneous case, using characteristic lengths of 5 m and 3 m (Figures 8 and 9 respectively).

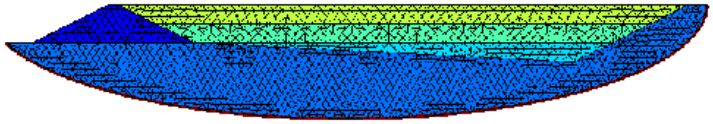

Figure 8. Coarse mesh

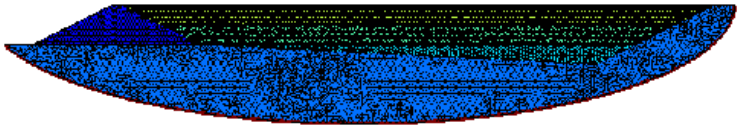

Figure 9. Fine mesh

To evaluate the effect of the mesh size, we selected an analytic Ricker wavelet with a peak time of 0.8 s, a pseudo-period of 0.2 s and amplitude of 0.1g. Figure 10 displays the Ricker signal and the corresponding Fourier amplitude. The Fourier spectrum shows that the wavelet delivers energy up to 12Hz, compatible with the typical frequency content of earthquake motions recorder on rock. The input motion is imposed by the paraxial elements after deconvolution from a control point placed on the hypothetical outcropping bedrock.

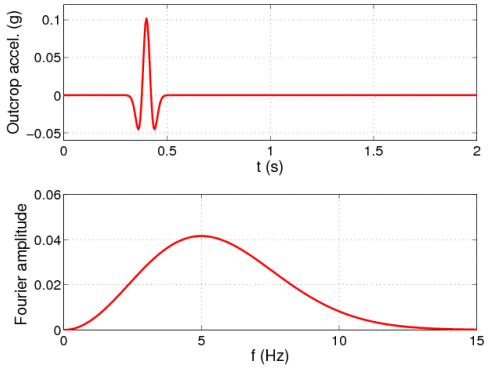

Figure 10. Ricker signal

Figure 11 shows the computed co-seismic settlement at the free surface of the deposit and the effect of the characteristic length on the results. The settlement time-history profile for the finer mesh seems more erratic because it includes a much larger number of nodes. The model whit a characteristic element length of 3m has 16500 elements, while the coarser model has ~3200 elements (a factor of ~5 in terms of the available amount of data).

Three control points were selected at the pond's surface to analyze their settlement time-history and to explore differences between both meshes. The selected points were located at a horizontal distance *y* of 50 m, 150 m and 200 m from the rockfill's top. Figure 11b shows the evolution with time of the vertical settlement of these points for the case of the coarse (dashed line) and fine (cointinuous line) mesh This analysis shows that the settlements time-histories are qualitatively very similar, with final differences around 10%. The finer mesh predicts larger values for the first and the second control points, while for the third control point the coarser mesh predicts larger results.

The previous analysis shows that a characteristic element length of 5 m is fine enough to reproduce the key aspects of the problem. Also, in terms of computing time, the coarser model requires ~1/5 of the times that the fine mesh needs to run.

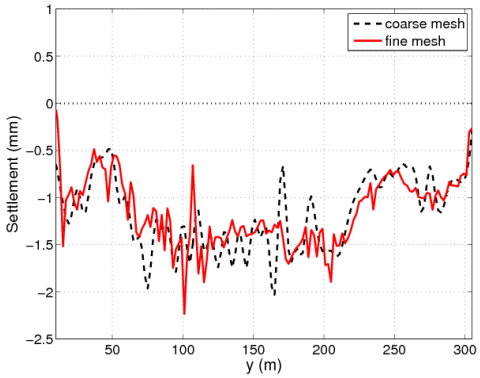

Figure 11a. Co-seismic settlement at the free surface of the deposit

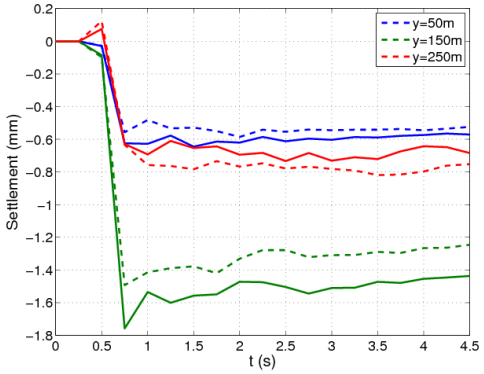

Figure 11b. Time-history settlement at three control points

4. DYNAMIC ANALYSIS

The influence of the desiccation cracks in the dynamic response of the deposit described in Section 2.1 was analyzed using a Chilean ground motion record, and considering both a homogeneous model and one with a larger permeability in the material between the desiccated blocks (Section 2.3). Due to the minimum width that was considered for the cracks (0.2m), the latter FE mesh is very fine (around 6500 elements), requiring more than 20 times the computer resources of the homogeneous case. For this reason, the results of a single realization of the randomly generated cracking pattern are presented in the following. As local amplification due to soil and geometry is directly included in the numerical model, only ground motions recorded in rock are suitable for the analysis. Among the available records, we selected the record of Rapel Station (NS component) recorded during the M7.8 March 3, 1985 Chile Earthquake (Riddell, 1995). This ground motion has a maximum amplitude close to 0.2g and a total duration of 80s approximately (Figure 12).

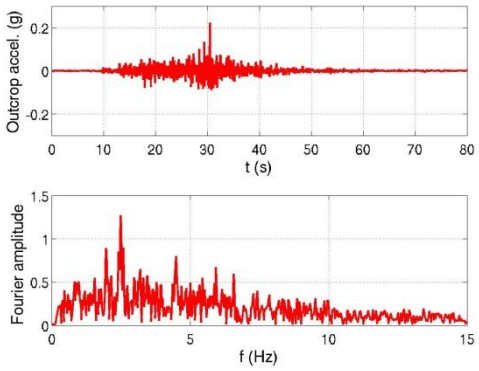

Figure 12. Seismic data used

Figure 13 shows the spatial distribution of vertical displacements u_z after 50s of analysis (negative values mean settlement). Figure 13a corresponds to the homogenous case, while Figure 13b corresponds to the case where desiccation cracks were included. The results using both approaches were very similar with a maximum settlement estimate about 20 cm. Also in both cases settlements were larger where the tailings deposit was thicker. Additionally, both models predict positive vertical displacements close to the rockfill crest. Computed values are close to 30 cm, i.e., larger than the maximum computed settlements. The authors believe that this "run-up" of the material over the rockfill is related to the massive settlement in the central portion of the deposit. If the material tends to settle in the central portion, and considering that the behavior of the TTDs during the earthquake is essentially undrained, the total volume change will be negligible and large settlements are likely compensated by vertical expansion in zones close to the rigid boundaries of the model. Nevertheless, note that a fully coupled approach was used in this analysis, and that undrained condition was s not enforced.

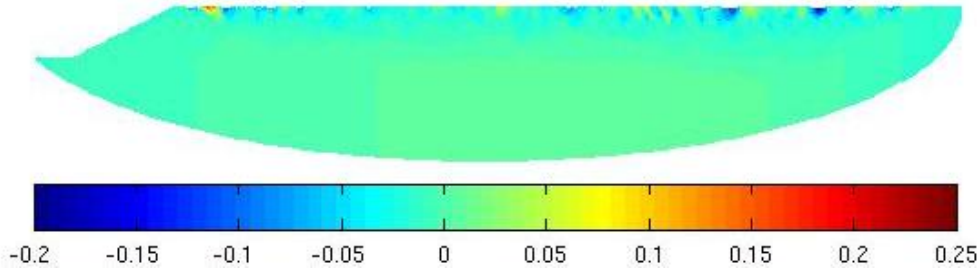

Figure 13.a Co-seismic settlements in meters assuming homogeneous material (t=50s)

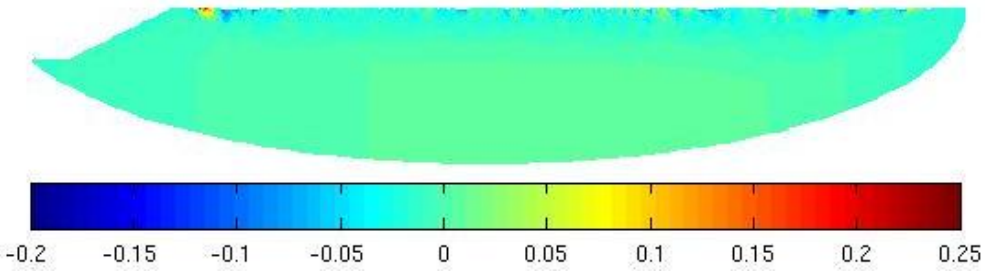

Figure 13.b Co-seismic settlements in meters including desiccation cracks (t=50s)

Finally the effect of the desiccation cracks on the liquefaction susceptibility of the deposit was evaluated. The ratio R_u between the pore pressure build-up Δp and the initial vertical stress $\sigma'_{zz}(t=0)$ at any point $\vec{x}$ inside the TTD, was used to illustrate the spatial distribution of liquefaction:

$$R_u(\vec{x},t) = \frac{\Delta p(\vec{x},t)}{\sigma'_{zz}(\vec{x},t=0)} \qquad (4.1)$$

Hence, as R_u approaches unity, pore pressure build-up gets close to the initial vertical stress and liquefaction at that this point begins.

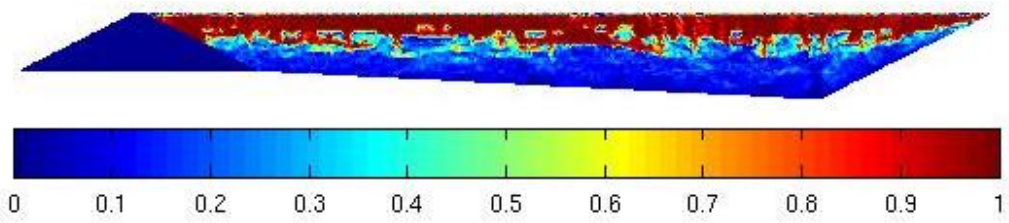

Figure 14.a R_u distribution assuming homogeneous material (t=50s)

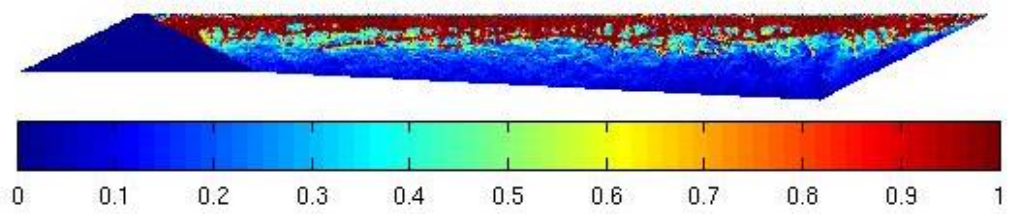

Figure 14.b R_u distribution including desiccation cracks (t=50s)

Figures 14a and 14b show, respectively, this Ru distribution, for the homogeneous and cracked TTD models at t=50 s. In both models full liquefaction takes place in the upper part of the deposit, where the material is poorly confined. A Slightly thinner liquefied layer is predicted for the cracked case when compared to the homogeneous case. Despite these differences, the overall conclusion is that the incorporation of the desiccation cracks on the model did not alter the general seismic behavior of the deposit significantly.

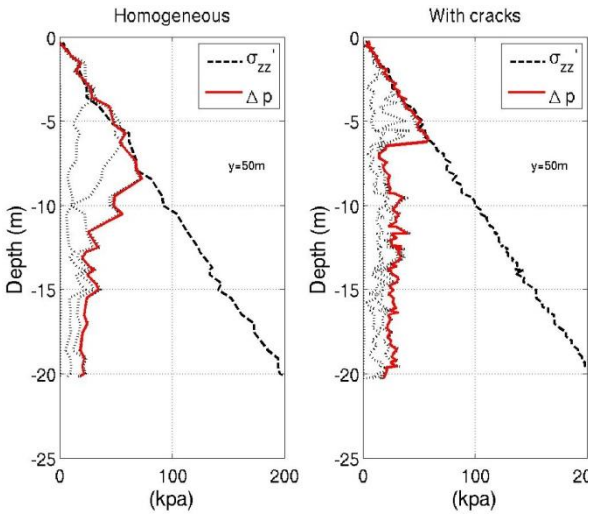

Figure 15.a Vertical stress/pore pressure increase profile at y=50m

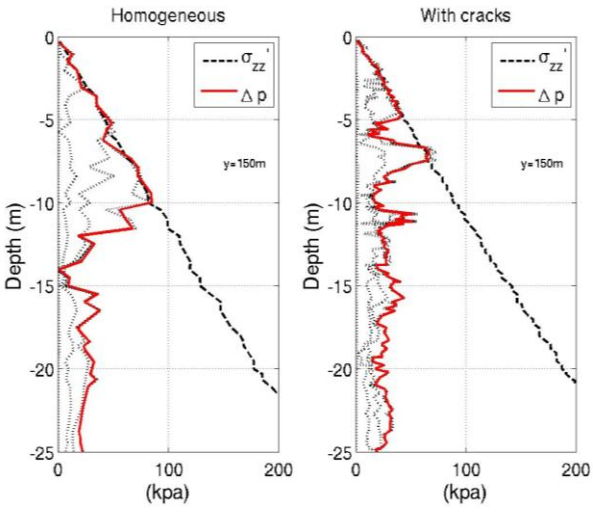

Figure 15.b Vertical stress/pore pressure increase profile at y=150m

Additionally, two vertical stress profiles at 50 and 150 m from the rockfill crest (see Figure 3) are shown in Figure 15. In these figures, the black dashed line corresponds to the initial effective vertical stress profile, the continuous red line is the final pore pressure buid-up profile (at 80 s) and the dotted lines are pore pressure increase profiles at 10, 20, 30, 40, 50 and 60 seconds. In all cases only the first two dotted lines can be distinguished, indicating that at 30 s of the analysis, liquefaction is completely developed. Regarding vertical extension, it is rather clear that liquefaction goes deeper when the material is assumed to be homogeneous. At 50 m of the rockfill crest, the liquefied layer reaches approximately 8 m deep in the homogeneous model, but when desiccation cracks are included, the liquefaction does not go below 6 m. The profile at 150 m from the rockfill crest shows a similar response. Additionally, when cracks are added to the model liquefaction zones becomes more "discontinuous", for instance, the superficial liquefied layer stops at 5 m meters deep, and another well-defined ~1 m appears at 7 m deep. In general, these analyses suggest that desiccation crack reduce the spatial extension of the liquefaction, but they do not prevent liquefaction from occurring. More realizations and computations needed to generalize these and others conclusions.

5. CONCLUSIONS

The main findings of the present work are:

- A new random-based procedure to generate desiccation cracks is proposed. This procedure can simulate occasional layer-to-layer desiccation's vertical continuity, which has been observed in real situations.
- Based on a mesh-size sensibility analysis using a homogeneous model, it was concluded that an element characteristic length of 5 m seems fine enough to reproduce the key aspects of this coupled dynamical problem.
- The inclusion of desiccations cracks to the FE model tends to reduce the spatial extension of the liquefaction in the studied problem. Nevertheless, these observations are related to a single random realization of the cracking distribution. More realization will be considered in the future to derive more general conclusions.

AKCNOWLEDGEMENT

The authors would like to thank MWH Global for their funding support. Discussions with Prof. Jorge Troncoso were very useful. Any opinion expressed in this material are those of the authors.

REFERENCES

Aubry, D. Hujeux, J-C, Lassoudière, F. And Meimon, Y. (1982) A double memory model with multiple mechanism for cyclic soil behaviour. *International sumposium on numerical models*. Balema: Geomech. 3-13.

Aubry, D. and Modaressi, A. (1996) GEFDyn: Manuel scientifique. Ecole Centrale Paris, LMSS-Mqt.

Cifuentes, L. (2010) Respuesta Monotónica y Cíclica no Drenada de un Relave Espesado. MSc Tesis, Universidad de Chile, Santiago, Chile.

Horgan, G. W. and Young, I. M. (1999). An empirical stochastic model for the geometry of two-dimensional crack growth in soil (with Discussion). *Geoderma*.

Hujeux, J-C (1995). Une loi de comportement pour le chargement cyclique des sols. Davidovici, V. Editor G'enie Parasismique. Presses ENPC. 278-302.

Ferrer, G. (2011). Estudio del Comportamietno Sísmico de Relaves Espesados Mediante el Análisis de Columna Unidimensional Considerando Grietas de Contracción. MSc Tesis, Pontificia Universidad Católica de Chile, Santiago, Chile.

Modaressi, H. and Benzenati, I. (1994) Paraxial approximation for poroelastic media. *Soil Dyn Earthquake Eng*, 117-29.

Nieto-Gamboa, C. (2011). Mechanical behavior of rockfill materials - Application to concrete face rockfill dams. PhD Thesis, Ecole Centrale, Paris.

Riddell, R. (1995). Inelastic design sprectra accounting for soil conditions, Earthquake Engineering & Structural Dynamics, Vol. 24, No 11, 1491-1510.

Robinsky, E. I. Thickened Tailings Disposal in the Mining Industry.
Verdugo, R. (2009). Seismic performance based-design of large earth and tailing dams, Performance-Based Design in Earthquake Geotechnical Engineering, ICPBD Conference, Tsukuba, Japan: 41-60.
Verdugo, R. (2011). Seismic Stability Analysis of Large Tailings Dams, 5th International Conference on Earthquake Geotechnical Engineering, Santiago, Chile.
Zienkiewicz, O., Shiomi, T., (1984) Dynamic behaviour of satured porous media: the generalized Biot formulation and its numerical solution. *Int J Numer Anal Methods Geomech*, 71-96.